We are IntechOpen, the world's leading publisher of Open Access books Built by scientists, for scientists

6,900
Open access books available

185,000
International authors and editors

200M
Downloads

Our authors are among the

154
Countries delivered to

TOP 1%
most cited scientists

12.2%
Contributors from top 500 universities



WEB OF SCIENCE™

Selection of our books indexed in the Book Citation Index in Web of Science™ Core Collection (BKCI)

Interested in publishing with us?
Contact book.department@intechopen.com

Numbers displayed above are based on latest data collected.
For more information visit www.intechopen.com



Chapter 10

Holographic Fabrication of Periodic Microstructures by Interfered Femtosecond Laser Pulses

Zhongyi Guo, Lingling Ran, Yanhua Han, Shiliang Qu and Shutian Liu

Additional information is available at the end of the chapter

http://dx.doi.org/10.5772/46136

1. Introduction

In recent years, with the developments of the laser technology, femtosecond laser technology is becoming more and more consummate as a novel technology. Femtosecond laser pulse is also becoming into a powerful tool for microfabrication and micro-machining of various multi-functional structures in dielectric materials through multi-photon absorption because of its high-quality and damage-free processing. Up to now, many high-quality material processing techniques have been achieved by using femtosecond laser pulses with the methods of directly writing [1-10] and holographic fabrication [11-22], such as waveguide [1], special diffractive optical elements (DOE) [4-10], micro-gratings [11-15], and photonic crystals [16-20]. Because multiphoton nonlinear effects play a major role in this process, the resulting change in refractive index or cavity formation can be highly localized only in the focal volume where the fluence is above a certain material dependent threshold, which makes it possible to micro-fabricate devices inside the bulk of transparent materials. These structures were usually fabricated with a focused beam and written dot by dot by translation of the sample with respect to the focal point.

Compared to directly writing technology by femtosecond laser pulses, holographic lithography has been considered as a more effective method for fabricating periodic structures because it can be controlled easily by the number of the beam, angles between every two beams, energies of the laser beams, and most importantly, only one pulse needed for holographic fabrication. Especially, holographic lithography is considered to be the most effective method for the fabrication of the photonic crystals. And Cai *et al.* [21-22] have proven that all fourteen Bravais lattices can be formed by interference of four noncoplanar beams (IFNB), and have quantitatively obtained the solutions including the required

INTECH
open science | open minds

© 2012 Guo et al., licensee InTech. This is an open access chapter distributed under the terms of the Creative Commons Attribution License (http://creativecommons.org/licenses/by/3.0), which permits unrestricted use, distribution, and reproduction in any medium, provided the original work is properly cited.

wavelength and the four wave vectors for each special lattice. The relative simulated results are shown in Fig. 1.

There are also many groups who have attempted to fabricate the periodic structures in photosensitive transparent materials or on the surface of the silica glass and the metal film by interfered multiple femtosecond laser pulses. Especially, it is very easy to fabricate the periodic structures inside of the photosensitive transparent materials with the aid of diffractive beam-splitter (DBS) [18-20]. However it is limited by the angles between two beams and the energy of the pulses. It is therefore difficult to fabricate microstructure with smaller period, especially in the materials with big band gap, such as silica glass. So there are also some researching groups [13, 16-17] focusing on the realization of periodic structures on the surface of the silica glass by a single shot of two or three femtosecond laser pulses originating from one pulse by the beam splitters.

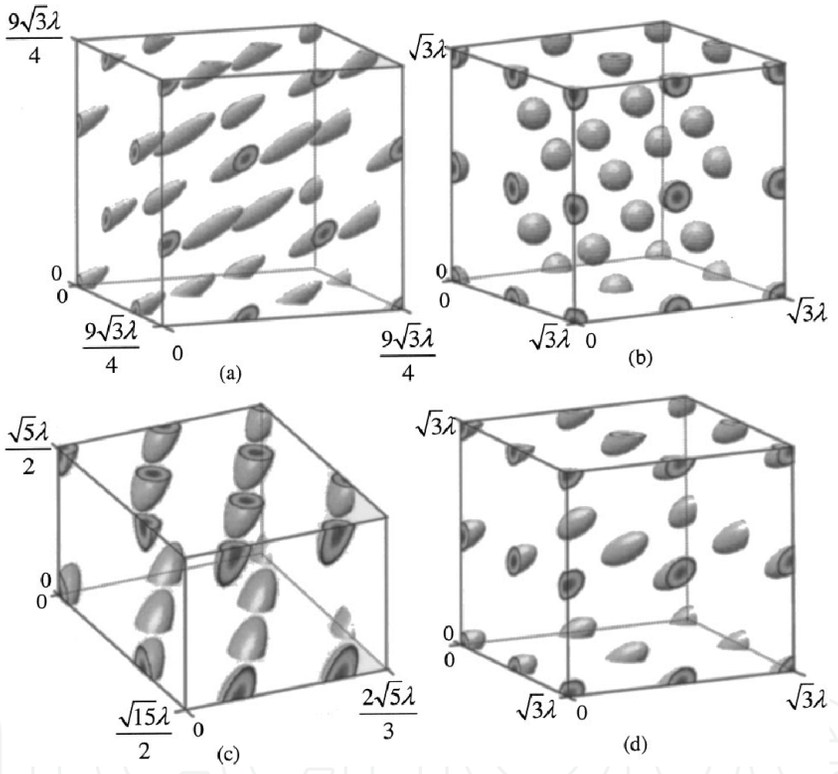


Figure 1. Computer simulations of four Bravais lattices formed by interference of four noncoplanar beams: (a) face-centered cubic lattice, (b) body-centered cubic lattice, (c) hexagonal lattice (c= 3a/2), and (d) simple cubic lattice.

In this chapter, we have reviewed the progress of fabrication of the periodic structures on the surface or inside of the transparent silica glass by a single shot of several (two, three, four) femtosecond laser pulses. When a single shot of two pulses interfered with each other, there will be one dimensional grating structures being formed inside of the photosensitive transparent materials or on the surface of the materials. When a single shot of three coplanar pulses interfered with each other, the one-dimensional M-shape grating can be formed on the surface of the silica glass. However, when a single shot of noncoplanar three or four

pulses interfered with each other, two-dimensional periodic microstructure can be obtained, which distributed as a hexagonal lattice or tetragonal lattice.

2. Holographic fabrication by a single shot of two femtosecond pulses

2.1. The formation of the common grating and the extraordinary grating on the surface of the silica glass

The experimental setup for the holographic fabrication of micrograting by a single shot of two interfered femtosecond laser pulses is depicted in Fig. 2 (a). A regeneratively amplified Ti:sapphire laser (Coherent. Co.) with a central wavelength of 800 nm, pulse duration of 120 fs, and pulse repetition of 1–1000 Hz was used. A single femtosecond laser pulse with a beam diameter of 6 mm could be selected and split into two pulses that were then redirected at controllable incident angles on the surface of the fused silica glass (K9 glass) which is transparent for the laser with a wavelength of 800 nm. These split pulses generating from the single pulse were focused on the glass surface by two lenses with focal lengths of 20 cm to give a spot size of ~50 μm at the focal plane. Attenuators could be used to obtain a proper energy of the pulses for controlling the results of the holographic fabrication. The two pulses could be adjusted both spatially and temporarily by the optical delay device perfectly. The angle between two pulse and the pulse energies could be controlled easily.

When we set the angle between the split beams as 40^o and the pulse energy as 45 μJ, the fabricated grating is shown in the Fig. 2 (b-e) by optical microscopy and atomic force microscopy (AFM) respectively. From the Fig. 2 (d), we can obtain the period of the fabricated grating is about 1.06 μm which agree well with the calculated result according to the formula $d=\lambda/[2\sin(\theta/2)]$ in which θ is colliding angle ($\theta=40^o$ in this experiment) between two incident beams and λ is the incident laser wavelength of $800\,nm$. The periods of the micrograting encoded by holographic technology should be controlled easily by varying the angle. Analogously, the depth of the fabricated grating could also be tuned by controlling the pulse energy.

However, when we set the angle θ as 20^o and the pulse energy as 65 μJ, the fabricated grating is shown in the Fig. 3. Not only did we get the ordinary grating whose periods accorded with the theoretic equation $d=\lambda/[2\sin(\theta/2)]$, but also obtained the extraordinary grating [15, 23] whose period is a half of the ordinary grating. The extraordinary grating formed at the middle of each bulge of the ordinary grating as shown in Fig. 3 (a-b), so the period of the extraordinary grating is a half of the ordinary grating's observed easily from Fig. 3(c) which also shows that the depth of the extraordinary grating is a half of the ordinary grating's nearly.

In the experiments, with the decrease of the incident energy in the same angle between two beams, the modulation depths of the extraordinary grating are decreasing gradually. With the increase of the angle between two beams with the same energy, the modulation depths of the extraordinary grating are also decreasing gradually. At last the modulation will be vanishing from the central part to the edge of the ordinary grating gradually.

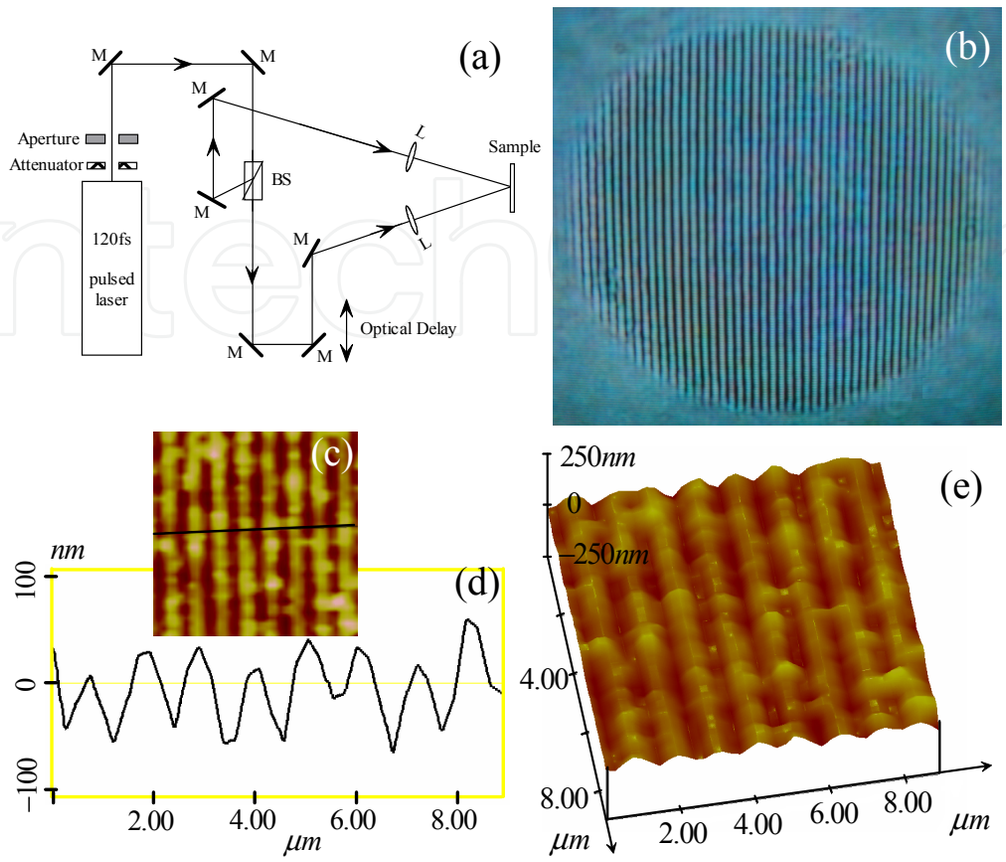


Figure 2. The experimental setup for the holographic fabrication of micrograting, (b) the fabricated grating observed by optical microscopy, (c) top-viewing AFM image of the fabricated grating, (d) cross-section view in the direction of black line shown in (c), (e) three dimentional view of the fabricated structure.

The formation of the modulation grating could be attributed to the higher-order modulation arising from second-harmonic generation (SHG) when the femtosecond laser pulse was incident to the surface of silica glass. As a rule, because of the inversion symmetry of the silica glass, there should be no second order nonlinearity in the silicon glass. However, a layer of plasma could be formed on the surface of the glass when the pulse incident to the sample because of the ultra high electrical field of the femtosecond laser in a time given by the duration of the laser pulse[24,25]. Therefore, when the femtosecond laser pulse with high intensity is incident on this thin plasma layer, there will be the higher harmonic generation because of the electrons quivering nonlinearly, and the SHG can reach to 2% of the fundamental laser [26]. The second-harmonic radiation is emitted in the direction of the reflected fundamental laser direction as depicted in Fig. 2 (d) [24]. So the period of the modulation grating is a half of the common grating because of the same of the angle between the two beams but a half of the wavelength. Although the intensity of the SHG is much smaller than the fundamental laser, the modulated depth of the silica glass can reach to a correspondingly large depth because it is much easier for the silica glass to be ionized by a mechanism of single or two photons absorption than multiphoton absorption.

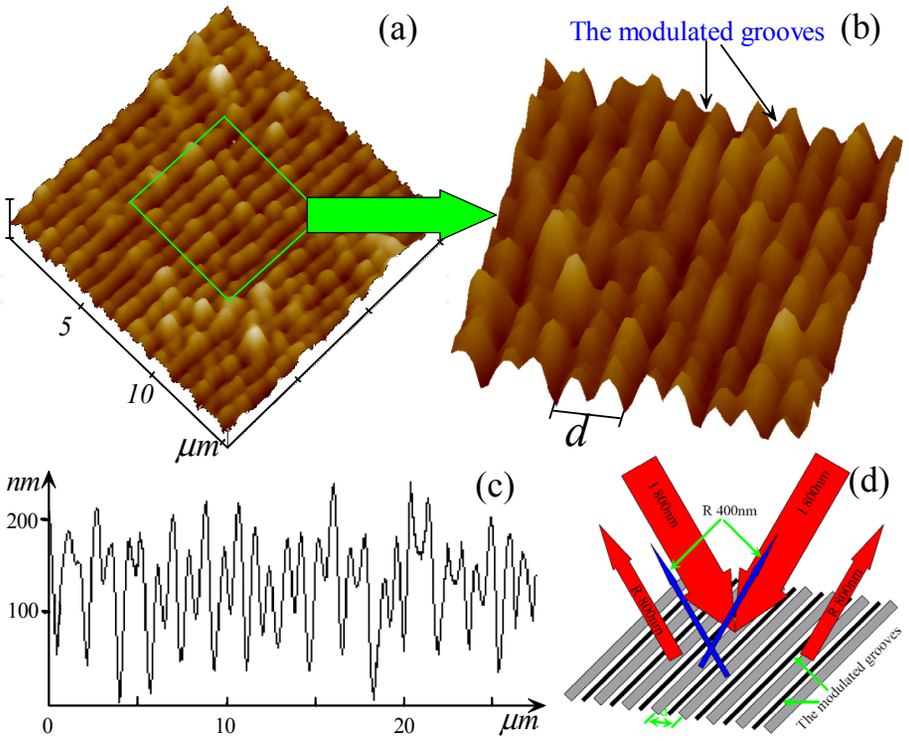


Figure 3. AFM photos of the resulted micrograting encoded with an energy of ~65 μJ for each interfered beam and a colliding angle of ~20°. (a) Image of the central portion of the grating, (b) an enlarged version for the chosen part in (a), and *d* is the period of the common grating. (c) cross-section view of the fabricated grating. (d) schematic illustration for the formation mechanism of the modulating grating.

2.2. Fabrication of multiple layers of grating

Li *et al.* [11] have reported that the multiple layers of grating can be fabricated inside soda–lime glass by a single shot of two interfered femtosecond laser pulses at different depths of the sample. A top view of experimental setup is shown in Fig. 4 (a), which is similar to the Fig. 2 (a). The two beams, with diameters of 5 mm, were focused by two lenses with focal length of 150 mm to give a spot size of 30 30μm at the focal plane.

The multiple gratings were written inside of the soda–lime glass one after another by focusing the beam 1 and beam 2 into special position inside of the glass sample with the recording plane. Without loss of generality, three layers of micrograting could be recorded at depths of 200, 400, and 600 μm, respectively. The grating at depth of 600μm should be encoded firstly. Then the sample was translated along the *z* direction to a depth of 400μm and the second grating could be recorded. After that, the third grating was fabricated after moving the sample to a depth of 200μm lastly.

Because the micrograting was formed inside of the samples around the focal point without damage to the surface or other parts of the sample, multiple layers of grating can be recorded successfully. And the images of the fabricated multiple layers of micrograting could be read out by beam 2 and taken over three different recording planes as depicted in

Fig. 4 (b) and (c). The schematics on the right illustrate the relative positions of the sample, three layers of grating, the recording plane, and the objective. The experimental results demonstrated that the readout image of the first layer (not shown here) and the second layer (as depicted in Fig. 4 (b)) of the recorded grating consisted of well-defined straight bright lines alternating with black lines. However, for the readout of the third layer of the micrograting, some of the straight lines became curved as shown in Fig. 4 (c). This aberration may be caused by the wave-front distortion of the incident beams due to the accumulation of nonlinear effects when the focused high peak-power pulse propagated through the sample. The longer the optical path inside the sample was, the more severe the wave-front distortion and the more obvious the resulting grating aberration.

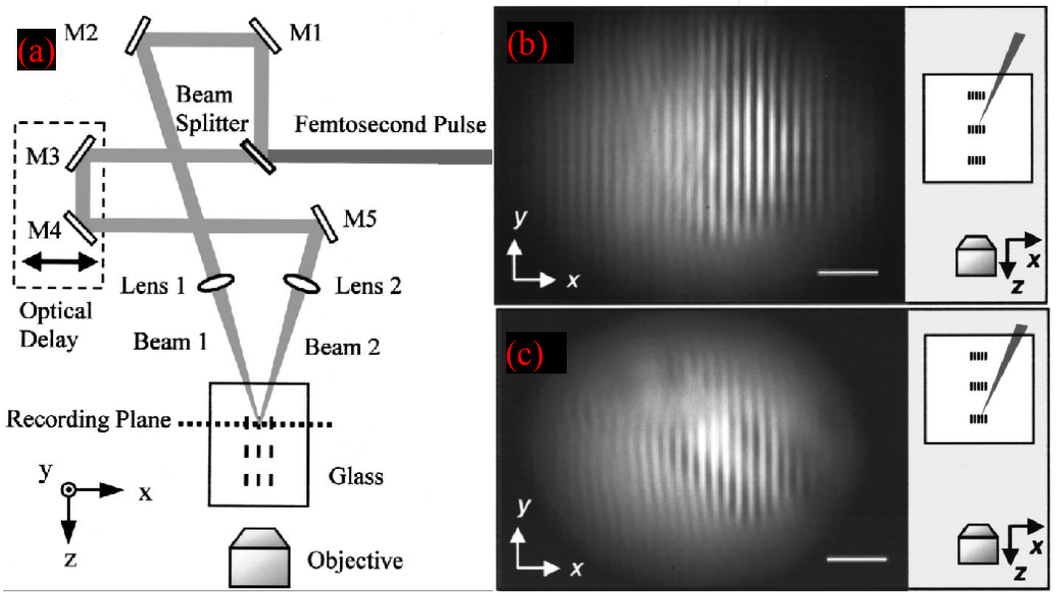


Figure 4. (a) Top view of the experimental setup for the formation of multiple gratings inside glass. The recording plane is in the $x - y$ plane and through the overlapping focal points of the two incident beams: beam 1 and beam 2. (b)(c). Readout images of the second and the third layers of grating inside a slide glass plate by beam 2. The images were taken through a 100X optical objective that was focused onto the recording planes at depths of 400μm (b) and 600μm (c) respectively. The schematics on the right indicate the relative positions of the sample, grating layers, the readout beam, and the 100X optical objective. Scale bar: 5μm.

2.3. Fabrication of micrograting inside the glass doped Au nanoparticles

Noble metal nanoparticle-contained glasses exhibit large third-order nonlinear susceptibility and ultrafast nonlinear response due to the local field effect near surface Plasmon resonance and quantum size effect [27, 28]. In recent years, many studies have been carried out on the fabrication of nanoparticle-doped glasses [29-31]. Shiliang Qu *et al.* realized the formation of micrograting constituted with Au nanoparticles in Au_2O-doped glasses induced by two interfered femtosecond laser pulses followed by successive heat treatment [12].

A typical silicate glass is composed of $70SiO_2.20Na_2O.10CaO$ doped with $0.1Au_2O$ (mol%). Reagent grade SiO_2, $CaCO_3$, Na_2CO_3, and $AuCl_3.HCl.4H_2O$ were used as starting materials.

An approximately 40g batch was mixed and placed into a platinum crucible. Melting was carried out in an electric furnace at 1550 °C for 1 h. The glass sample was obtained by quenching the melt to room temperature. The sample thus obtained was transparent and colorless. The annealed sample was cut and polished, and then subjected to successive experiments for femtosecond laser.

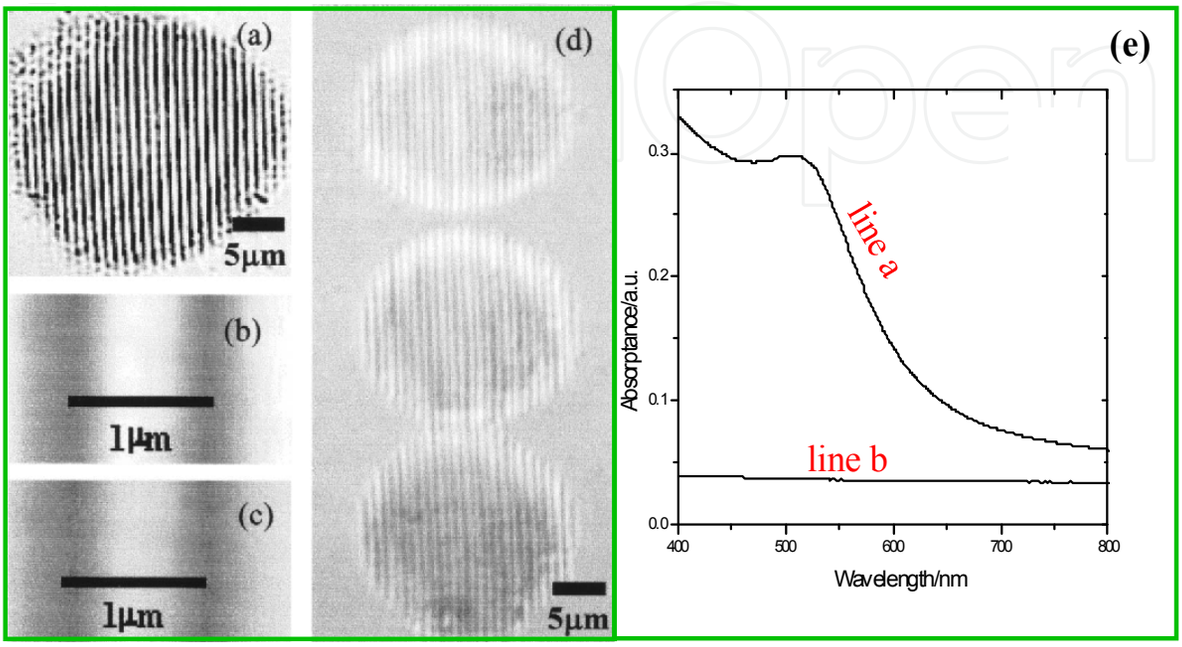


Figure 5. Optical microscopic photos of Au nanoparticles precipitation in periodic arrays in silicate glass (micrograting), taken by a 100X transilluminated optical microscope. (a) Energy is 30 μJ per pulse. (b) Magnified view of (a). (c) Energy is 38μJ per pulse. (d) Part of a group of formed micrograting array inside of the sample. (e) Absorption spectra of the glass samples after holographic irradiation by femtosecond laser pulses with (line a) and without (line b) heat treatment.

The used laser system and the experimental setup are the same as the used setup as shown in Fig. 2 (a). The two incident beams were first focused onto the front surface of Au_2O-doped glass to optimize the incident pulse energy. In the case of sufficiently high energy, the two coherent beams can induce periodic ablation, forming a grating in the glass. Herein, we reduced the incident pulses' energy to a certain lower level at which the two coherent beams cannot directly induce periodic ablation on the surface of the glass. Then the sample was moved 50μm to the lens in the direction of angular bisector of two incident light paths and made the laser pulses be focused inside the glass. After irradiation by a single shot of two interfered pulses, the micrograting can be recorded inside the glass, which can not be observed immediately because there is no obvious changes in the focusing place, however, after heat treating the sample at 550 °C for 1 h, the formed micrograting can be observed because of the Au nanoparticle precipitation. Such grating was constituted by the laser-heating induced Au nanoparticle precipitation in the Au_2O-doped glass.

In Qu's experiments, this lower pulse energy was selected to be 30 and 38 μJ for comparison, and the colliding angle θ between the two incident beams was fixed at 45°. The fabricated

micrograting is shown in Fig.5 (a-d). The period d of the obtained gratings was about ~1μm which was agreeing well with the value calculated from the colliding angle θ and the laser wavelength λ according to the formula $d=\lambda/[2\sin(\theta/2)]$.

The absorption spectrum of the grating was measured by a spectrophotometer (JASCOV-570) as shown in Fig. 5 (e) (line a). Apparently, a weak peak occurs around 508 nm, which is induced by the surface plasmon resonance of Au nanoparticles in the glass. The Au nanoparticles with 3 nm average size in the glass were observed in the grid of the fabricated micrograting from a transmitted electronic microscopy (TEM). However, if the glass sample was irradiated only by the interfered pulses but not heat treated, neither could absorption peak in the range of 500–600 nm be observed in the absorption spectrum as shown in Fig. 5 (e) (line b), nor could Au nanoparticles be observed by the TEM. This indicates that the Au nanoparticles can be precipitated in the periodic one-dimensional arrays in the glass through the irradiation of two coherent beams with the aid of heat treatment.

2.4. Fabrication of multiple gratings by a single shot of two interfered femtosecond laser pulses

The interference of two laser beams can create microstructures with one-dimensional periodic patterns in certain materials due to the periodic modulation of the laser intensity with a period scale of the order of the laser wavelength. As stated as above, there has been many groups focusing the fabrication of microgratings in glasses [11, 12], thin films [32], polymers[33], and inorganic–organic hybrid materials [34] by use of two interfered femtosecond laser pulses in a single shot. However, there is a disadvantage for micrograting fabrication with this method: Only a single micrograting can be formed for one pulse. Shiliang Qu *et al.* have reported holographic fabrication of multi-microgratings on silicate glass by a single shot of two interfered femtosecond laser beams with the aid of a mask [14].

In the experimental setup as shown in Fig. 6 (a) which is similar with the Fig. 2 (a) and Fig. 4 (a), a regeneratively amplified Ti:sapphire laser (Spectra-Physics) with a wavelength of 800 nm, pulse duration of 120 fs, and pulse repetition of 1–1000 Hz was used. A single laser pulse with a beam diameter of 8 mm was selected and split into two beams that were then redirected at approximately equal incident angles on a silicate glass surface. The two beams were focused on the glass surface by two lenses with focal lengths of 10 cm (L1) and 20 cm (L2) to yield spot sizes of 40μm and 80μm, respectively.

The colliding angle θ between the two beams was fixed at 40^{o}. After the optical paths were adjusted to realize perfect overlap of the two beams both spatially and temporally, the surface of the glass was adjusted to be approximately normal to the perpendicular bisector of the two incident beams, so that the glass surface became the laser interfering plane. A mask used for laser beam modulation was placed in the optical path in which lens L1 is located. The mask consists of three equilaterally and triangularly arrayed apertures, whose diameters are 2.5 mm and the spaces between them are 3.5 mm as shown in Fig. 6(b).

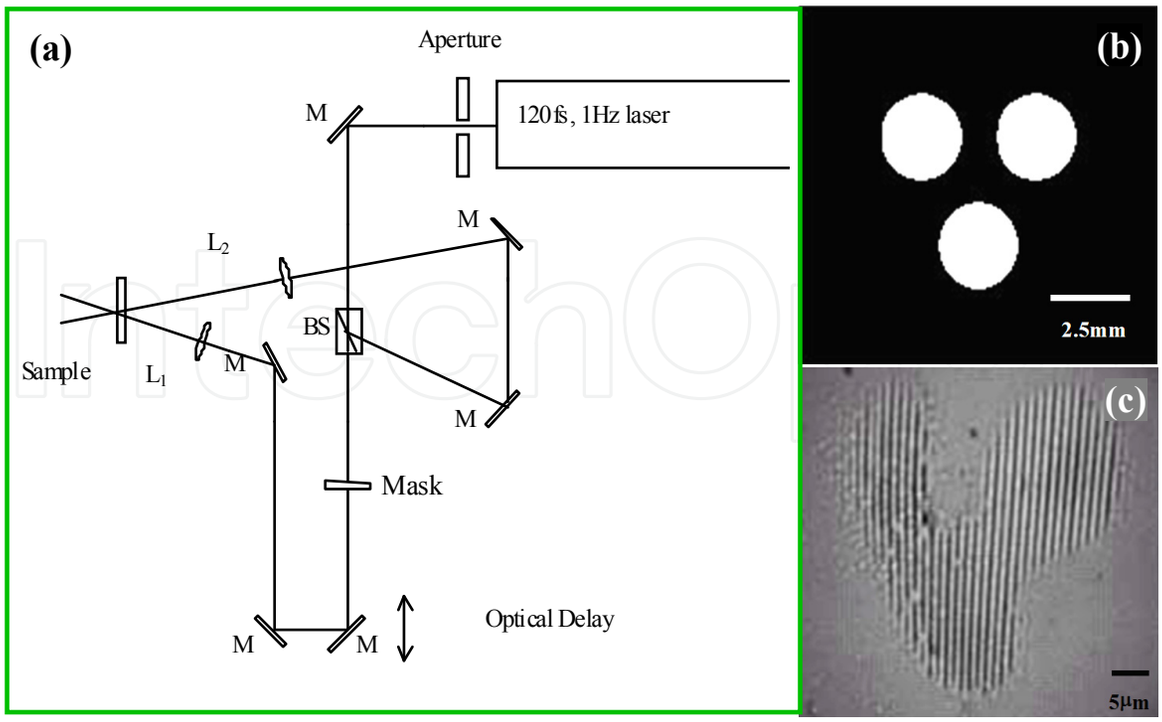


Figure 6. Experimental setup for the one-off writing of multi-micrograting by a single shot of two femtosecond laser pulses. M's, mirrors; BS, beam splitter. (b) Data mask for multimicrograting formation. (c) Optical microscopic observation of a multi-micrograting formed on silicate glass with a period of 1.1μm ($E_{1,2}$~70 μJ, θ~40°).

After irradiation by one single shot of two interfered pulses, the multi-micrograting comprises three micrograting as shown in Fig. 6(c), which has a high fidelity to the configuration of the mask used. The multi-micrograting was formed through periodic ablation resulting from the interference of the reference laser beam with the three beams caused by the mask. And the period of the formed micrograting is also agree well with the theoretical expectation of the common grating $d=\lambda/[2\sin(\theta/2)]$. This means that a multi-micrograting comprising even more micrograting and configurations can also be one-off written by changing only the mask structure. However, multi-micrograting formation can be realized only when the two interfered beams are overlapped at an appropriate position out of their focus on the front surface of the glass.

3. Holographic fabrication by a single shot of multiple femtosecond pulses

3.1. The formation of the M-shaped micrograting by three coplanar interfered beams

As stated above, two interfered femtosecond pulses' interference can induce one and two-dimensional periodic structures by single and double-exposure techniques, respectively [11–15, 40]. However, usually the second pulse could not overlap completely with the microstructure formed by the first pulse in the double-exposure technique due to the rather

small size of the focal spot. Here, we will show that the fabrication of M-shape gratings with controllable modulation depth could be realized by adding the third beam into a two-beam interference system. The experimental results show that the depth ratio between neighbor grooves can be conveniently controlled by changing the pulse energy of the third beam. Morphology characterizations of as-fabricated periodic M-shape gratings with a period of 2.6 μm are presented by optical microscopy and atomic force microscopy (AFM). A theoretical simulation has also been done for explaining the concrete experimental results, which shows a higher fidelity to the experiment.

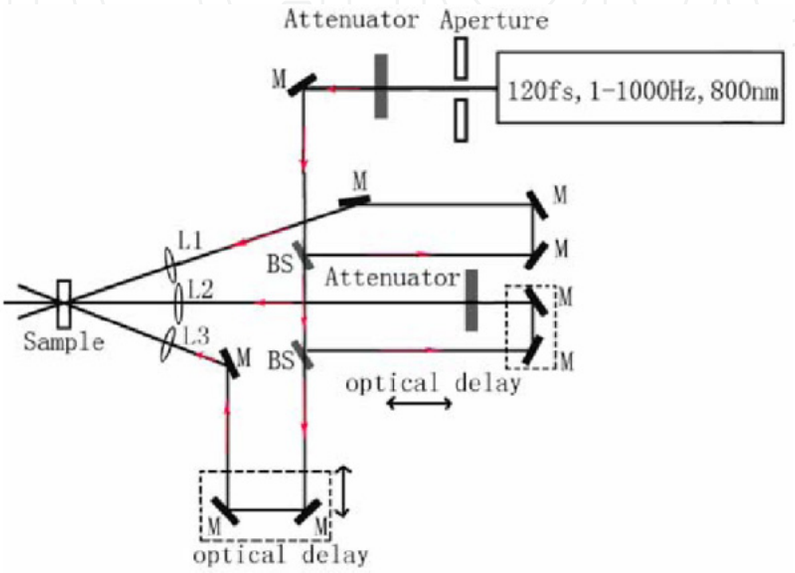


Figure 7. Experimental setup of three-beam interference optical system (AT and AP stand for attenuator and aperture, respectively).

The schematic experimental setup for fabricating M-shape grating is shown in Fig.7. The used ultrafast pulses (with a pulse width of 120 fs, central wavelength of 800 nm, and repetition rate of 1–1000 Hz) are produced by a Ti: sapphire regenerative amplified laser system (Coherent Inc). A laser pulse with a diameter of ~5 mm is split into three beams by two beam-splitters. Then three beams are focused by three lenses (L1; L2, and L3), each with a focal length of 150 mm, to give a spot size of ~50 μm at the focal plane. The collision angles between L1–L2, L2–L3, and L1–L3 are θ, θ, and 2θ (θ = 18◦ and 30◦), respectively. Two time-delay devices are employed for time adjustment of the beams collision. A BBO frequency-double crystal is located at the focal spot to check time superposition by SHG. When three collinear blue points appear on the white screen located on the back of frequency-double crystal, it indicates that three beams have been superposed on each other both spatially and temporarily. Two attenuators are used to adjust the energy of femtosecond laser pulse. The sample silica glass is located in the direction perpendicular to beam L2.

The optical microscope images of the gratings formed on the silica glass at different pulse energies of L2 (θ = 18◦, the pulse energies of L1 and L3 are both 50 μJ) are shown in Fig. 8 (a) and Fig. 8 (b). The neighbor grooves with different widths alternatively can be observed in

the grating as shown in Fig. 8 (a). However, in Fig. 8 (b), the neighbor grooves of the as-formed grating have the same widths. Fig. 8 (c) shows the AFM characteristic results of as-formed grating (in Fig. 8 (a)). Fig. 8 (c) is a top-view AFM image of the formed micrograting, where the neighbouring grooves with different widths alternately appear more clearly. Fig. 8 (d) displays the three dimensional morphology, which clearly shows that the M-shape grating is formed by the alternate appearing of two kinds of grooves: the deeper grooves and the shallower grooves. Fig. 8 (e) indicates a cross-section scanning picture along the horizontal line 'L' shown in Fig. 8 (c).

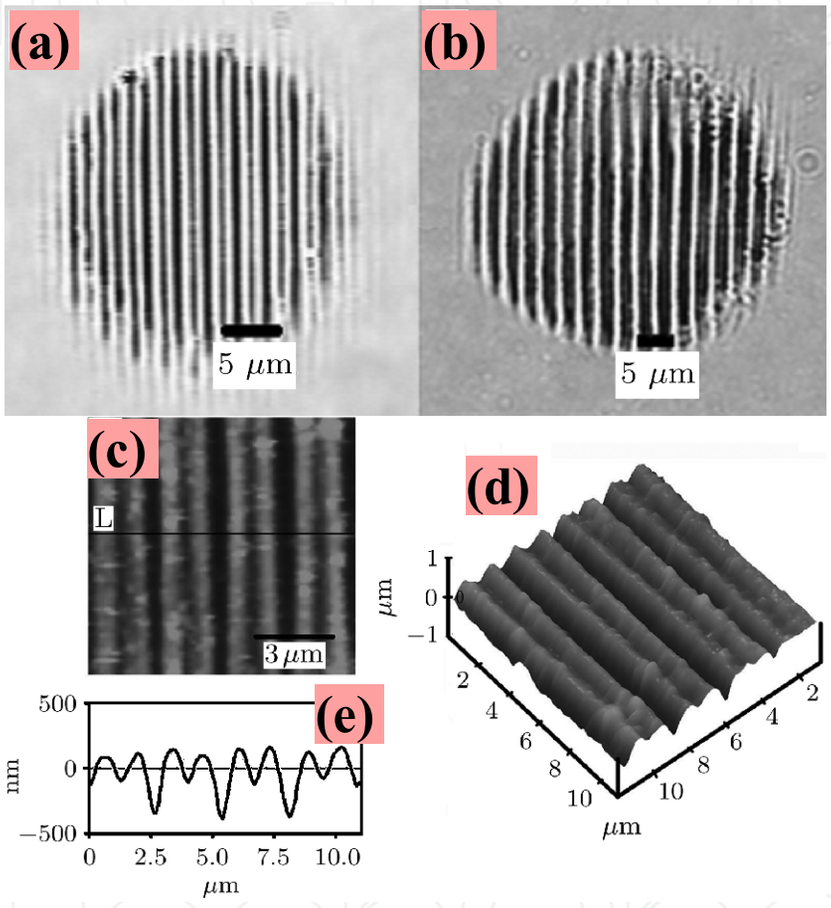


Figure 8. Optical microscope images of as-formed gratings by coplanar three-beam interference with different pulse energies of L2, i.e. (a) 50 μJ and (b) 100 μJ. AFM images of the M-shape grating formed on silica glass by three coplanar interfering beams, each with equal energy of 50 μJ, the collision angles of three beams are 18◦, 18◦, and 36◦, respectively. Panel (c) is for planar image, panel (d) for three-dimensional image, and panel (e) for cross-section pattern along line L.

It is obviously shown that the structure is formed by periodically arranging the M-shape units with a size of about 2.6 μm. The modulation depths of the deeper grooves and shallower grooves of the M-shape grating are ~500 nm and ~240 nm, respectively. The deeper grooves and the shallower grooves of the M-shape grating each have a period of ~2.6 μm revealed in Fig.8 (c). This result accords well with the value calculated from the universally known period formula $d = \lambda/\sin\theta$ (in our case λ = 800 nm, θ = 18◦, and d = 2.59 μm).

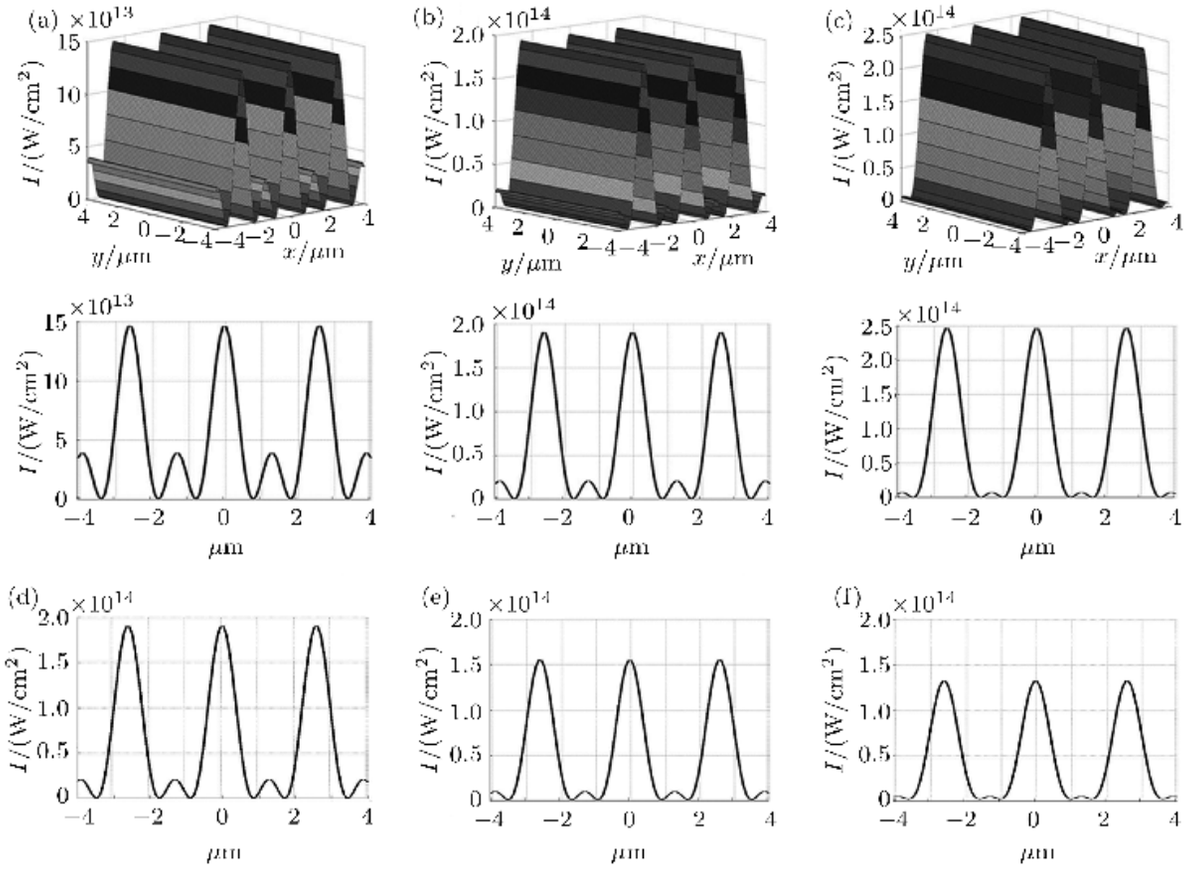


Figure 9. Intensity distributions simulated by using three interfering coplanar beams with different pulse energies of L_2 ((a), (b), and (c)) and L_3 ((d), (e), and (f)), where $k = 2\pi/\lambda$, $\lambda = 800$ nm, $\theta = 18^\circ$ and different values of I_{01}, I_{02} and I_{03}, i.e. (a) $I_{01} = 2.12$, $I_{02} = 0.85$, and $I_{03} = 2.12$, (b) $I_{01} = 2.12$, $I_{02} = 2.12$, and $I_{03} = 2.12$, (c) $I_{01} = 2.12$, $I_{02} = 4.24$, and $I_{03} = 2.12$, (d) $I_{01} = 2.12$, $I_{02} = 2.12$, and $I_{03} = 2.12$, (e) $I_{01} = 2.12$, $I_{02} = 2.12$, and $I_{03} = 1.06$, and (f) $I_{01} = 2.12$, $I_{02} = 2.12$, and $I_{03} = 0.53$, which are all in units of 10^{13} W/cm^2.

The simulated intensity distributions in the interfering region formed by three coplanar interfering beams are shown in Figs. 9 (a), (b) and (c), which correspond to the middle beam (L2) pulse energies of 20 μJ, 50 μJ and 100 μJ, respectively. In Figs. 9 (a), (b) and (c), the upper images show the three-dimensional patterns and the nether curves display the two-dimensional cross-section patterns. From the cross-section images of Figs. 9 (a-c), we can see clearly that the periodic intensity patterns are formed by the periodic arrangement of inversely M-shape structures, which is attributed to stronger intensity peaks and weaker ones arrayed with the same period of about 2.6 μm alternately and periodically. These results are consistent with the AFM results as shown in Fig. 8. We notice that with the energy of the middle pulses increasing, the stronger intensity peaks in the interfering region increase, while the weaker intensity peaks decrease. It indicates that the intensity ratio of the stronger peak and the weaker one increases. If laser pulses with such a periodic inversely M-shape intensity distribution irradiate the materials, the stronger intensity peaks will lead to the formation of deeper grooves, and the weaker intensity peaks will induce the formation of shallower ones. As a result, the M-shape surface structures will be resultantly formed. This fabricating technology for the formation of M-shape gratings provides a

fabricating method for special gratings with special use in industrial applications, such as the calibration for 3D reconstruction in computer vision application. And the fabricated M-shape grating can also be used in microfluidic chip devices as transport channels with different flowing speeds.

3.2. The formation of the triangular lattice by three noncoplanar interfered beams

When a single shot of three coplanar pulses interfered with each other, the M-shaped gratings could be fabricated as above. However, when a single shot of three non-coplanar pulses interfered with each other as depicted in Fig. 10 (a) by adjusting two time-delay for obtaining perfect overlap of the three pulses both spatially and temporarily, the two-dimensional periodic microstructure have been obtained, which distributed as a hexagonal lattice as shown in Fig. 10 (b) and agreed well with the simulated results [see Fig. 10 (c)] [16, 17]. In experiments, the geometric angles were kept as $\theta=30^0$ and $\varphi=35^0$ respectively as shown in Fig. 10 (a). When we set the pulse energy as 75 μJ, we can obtain two-dimensional periodic hexagonal lattice of microholes [see Fig. 10 (d-f)], however, when we set the pulse energy as 30 μJ, the two dimensional periodic microstructures present doughnut orbicular platform [see Fig. 10 (g-i)]. The period in the direction of line "*L*" is nearly 2.358 μm according to Fig. 10 (f) and (i) which agrees well to the calculated result [16].

The different microstructures in our experiments were attributed to the formation of plasma and molten liquid at different pulse energy levels. Generally it is hard to form plasma and molten liquid on the surface of silica glass by a laser with a wavelength of 800 nm because of the bigger band gap. However, the intensity at the focal point of the femtosecond laser beam where three beams interfere together could reach to 100 TW/cm^2 nearly. Such a high-energy influence within the focal volume ionized the silica glass quickly through the combined action of the avalanche and multiphoton processes [17, 35]. A layer of plasma formed on the surface of the silica glass at the time of the laser pulse duration. While the intensity decreased to be lower than a certain value, which can be called the ionized threshold as shown in Fig. 11 (a), the plasma vanished and the molten liquid of the material appeared. With the decrease of the intensity to be lower than a certain value, which could be called the molten threshold [see Fig. 11 (a)], the molten liquid of the material disappeared, so there would be a doughnut molten liquid formed in every enhanced spot of the interfered field [see Fig. 11 (b)]

When the pulse energy was set as 75 μJ, a layer of modulated plasma was formed by the interfered field with hexagonal lattice depicted in Fig. 10 (c) after the anterior part of the pulse was incident to the surface of the silica glass. Higher intensity induced a relatively larger plasma area in every enhanced spot of the interfered field. The subsequent posterior part of the pulse removed the plasma very swiftly because of the high light pressure originating from the reflection. Therefore, the microholes formed on the surface of the silica glass, as depicted in Fig. 10 (d-f). When the pulse energy decreased to 30 μJ, there was just a layer of the plasma with smaller areas than that of 75 μJ in the center of every enhanced spot in the interfered field after the anterior part of the pulse was incident to the surface. The

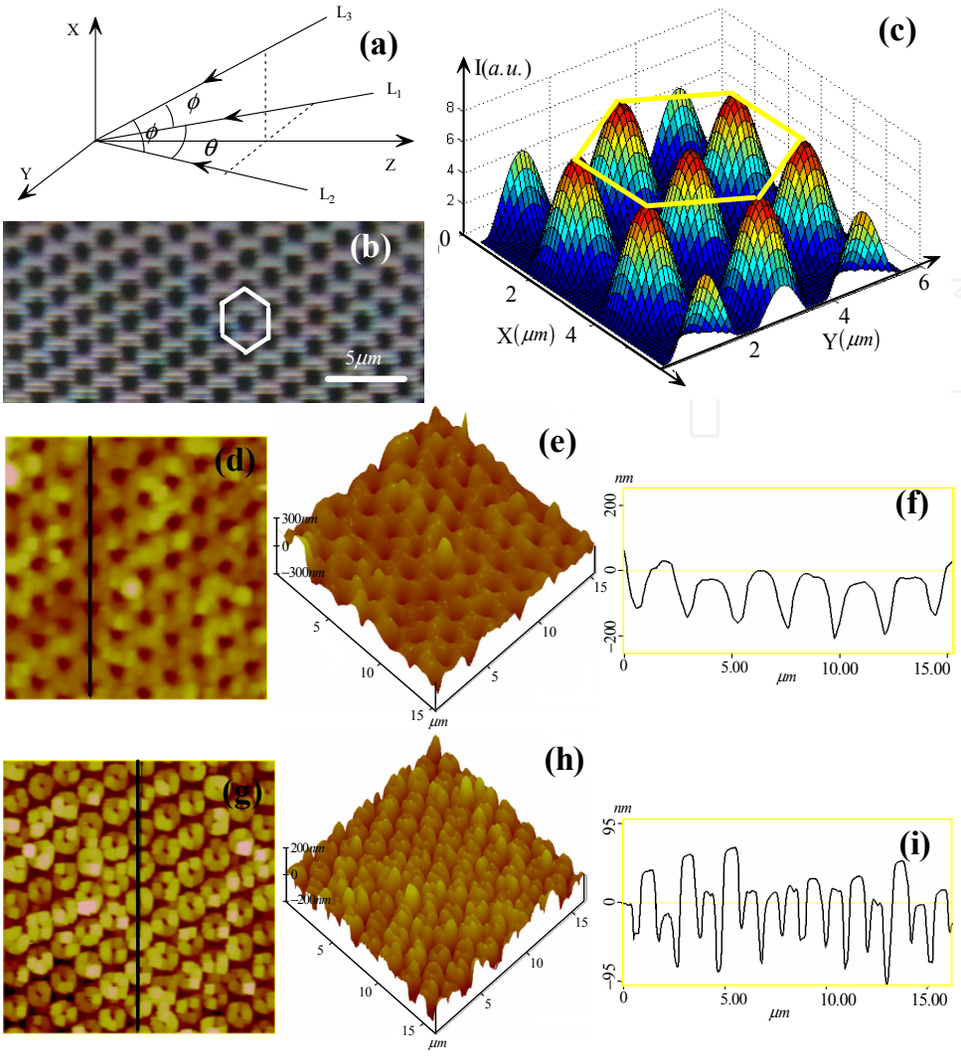


Figure 10. (a) Geometric sketch of the three non-coplanar interfered beams, and the sample is laid in the *x*–*y* plane, (b) Photo of the periodic microstructure fabricated in silica glass, taken by an optical microscopy, (c) Calculated intensity distribution of the interference by three non-coplanar beams. The induced periodic microstructure depicted by an AFM: (d) Energy is 75 μJ per pulse, (g) Energy is 30 μJ per pulse, (f) (i) Three-dimensional image of the microstructure of (d) and (g) respectively, (e) (h) The cross section of the microstructure in the direction of black line showed in (d) and (g) respectively

subsequent posterior part of the pulse also removed the central plasma very swiftly by means of light pressure, so there is a tiny hole formed in the center of the enhanced spot. However, in the region of the molten liquid, there were two distinct interaction components because of Marangoni effect, thermocapillary and chemicapillary, which resulted from the thermal potential of a temperature gradient and the chemical potential of a compositional gradient, respectively [17, 36-37]. The thermocapillary force moved the molten material outward from the center, while the chemicapillary force moved the molten material toward the center [38-39] as depicted in Fig. 10 (b). When the chemicapillary force dominated, a platform formed in the center of the spot. The combined action of the light pressure to the plasma and the chemicapillary force to the molten liquid induced a periodic orbicular platform on the surface of the silica glass as depicted in Fig. 10 (g-i).

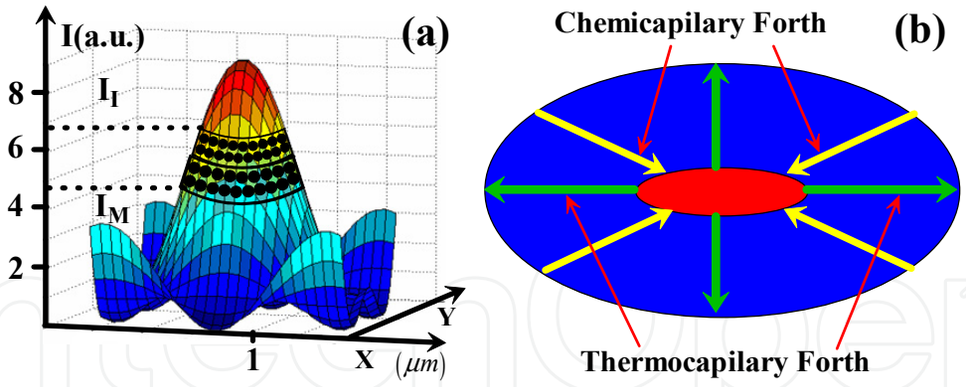


Figure 11. (a) The intensity distribution of the enhanced spot in the interfered field by three non-coplanar beams, I_I and I_M represent the densities of the ionized and molten thresholds respectively, (b) schematic diagram explanation for the mechanism of formed different structures owing to the formation of the plasma and Marangoni effect.

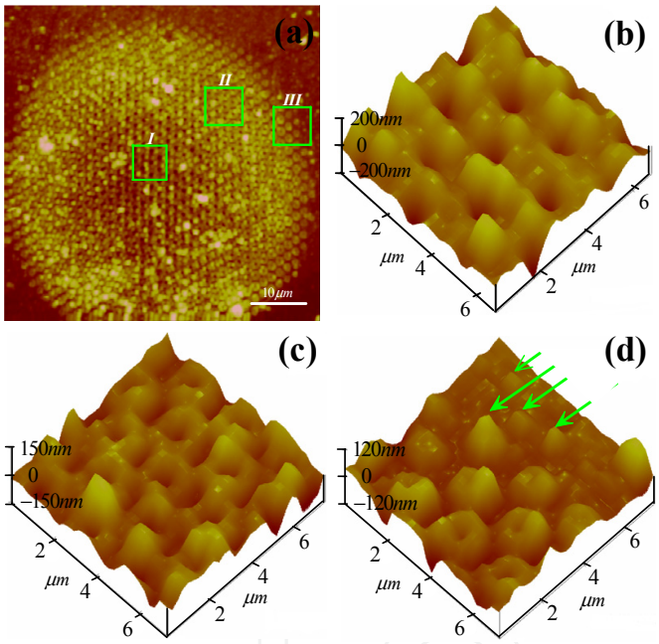


Figure 12. (a) AFM photo of the periodic structure induced by a single shot of three pulses with pulse energies of 50 μJ. Three-dimensional analyzed photos of the three selected parts I, II, and III in (a) are shown in (b)–(d) respectively.

In order to verify our explanation on the different induced microstructures, we set the pulses energy as 50 μJ, and the resulted microstructure is shown in Fig. 12 (a). Because of the Gaussian type intensity distribution of the pulse, three regions are selected from the central part (I), outer part (II) and the edge part (III) of the microstructure as depicted in Fig. 12 (a). The corresponding three dimensional images of the selected areas are shown in Fig. 12 [(b)-(d)], respectively. For the region I, the intensity is high enough to make the light pressure dominate, therefore the periodic microholes formed [see Fig. 12 (b)]. In contrast, in the region II, where the intensity is comparatively low, the chemicapillary force and the light pressure dominate, so that the microstructure present a orbicular platform [see Fig. 12 (c)].

However, in the selected area III, the intensity is very low and there is no plasma layer but just a layer of liquid formed on the surface of the silica glass. In this case, if the chemicapillary force dominates, the microcones can be observed. As shown in Fig. 12 (d), just several microcones (indicated by arrows) formed in the edge of the interfered districts.

3.3. The formation of the tetragonal lattice by four noncoplanar interfered beams

The interference of two beams creates a one-dimensional (1D) periodic pattern. By increasing the number of beams [16-20] or the double-exposure techniques [40], in principle, two-dimensional (2D) and three-dimensional (3D) periodic patterns can be designed. Although, as stated above, the interference of the three beams [13, 16-17] can create a 1D [13] or 2D [16, 17] periodic pattern on the surface of the materials of inside the transparent materials, the complicated optical setup is required for the interference of multiple laser beams, and its precise adjustment is difficult. Kondo *et al*. [18, 19] and Si *et al*. [20] have reported the fabrication of the 2D tetragonal lattice by four noncoplanar interfered pulses originating from the single pulse with the aid of the special DBS (diffractive beam splitter).

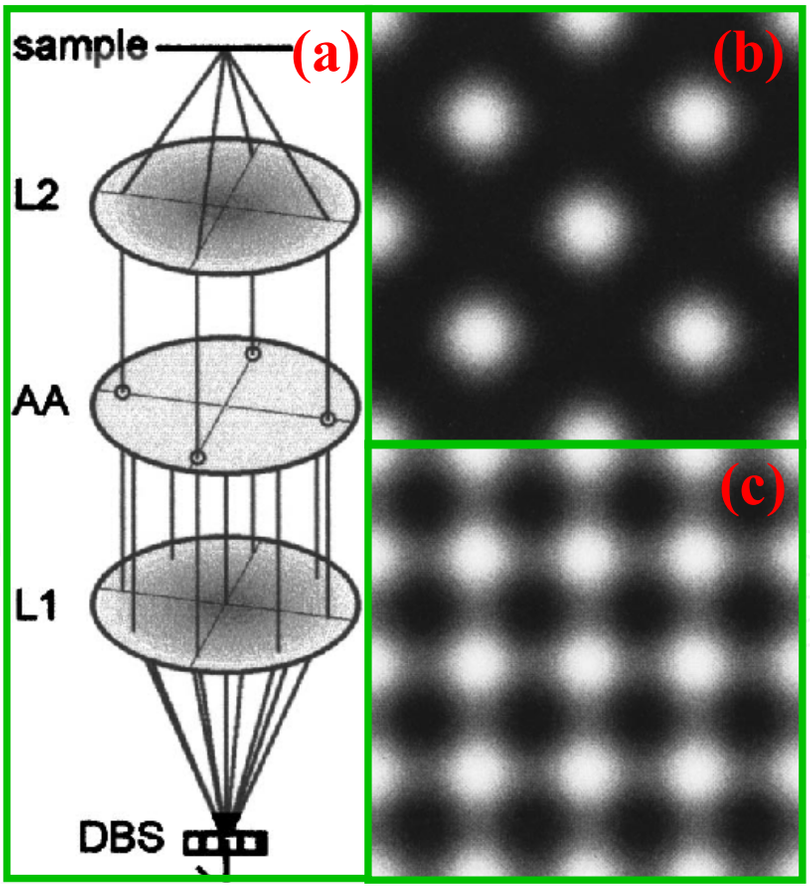


Figure 13. (a) Optical setup. DBS: diffractive beam splitter, L1 and L2: lenses,AA: aperture array. The inset shows the absorption spectrum of 4-mm-thick SU-8 film spin-coated on a coverglass. (b) Calculated intensity distribution by the interference of four beams which have same phase, (c) phase of one beam is shifted by π.

The optical setup used for the present experiments is shown in Fig. 13(a). Briefly, a DBS (G1023A or G1025A; MEMS Optical Inc.) divides the input laser beam into several beams, and the beams are collected on the sample by two lenses. Temporal overlap of the divided pulses is achieved without adjusting the optical path lengths. Each beam was made to be parallel or slightly focused by the adjustment of the distance between the two lenses. Slight focusing increased laser power density and helped to make the MPA efficient. The beams meant to form interference were selected by an aperture array, which is placed between the two lenses. Negative photoresist SU-8 (Microlithography Chemical Corp.) was used as an initial material for the fabrication. The absorption spectrum of SU-8 indicates that one-photon absorption is negligible at an 800-nm wavelength. Consequently, it is expected that photopolymerization, if occurring, is due to a multiphoton reaction. The layer of SU-8 was spin-coated on a coverglass plate having a thickness of about 4 μm, and prebaked before exposure to fs pulses. The interference angles θ_{air} (the angle between the main optical axis and the other beams in air) applied in the experiments were measured to be 33.6°, 21.9°, and 10.8°.

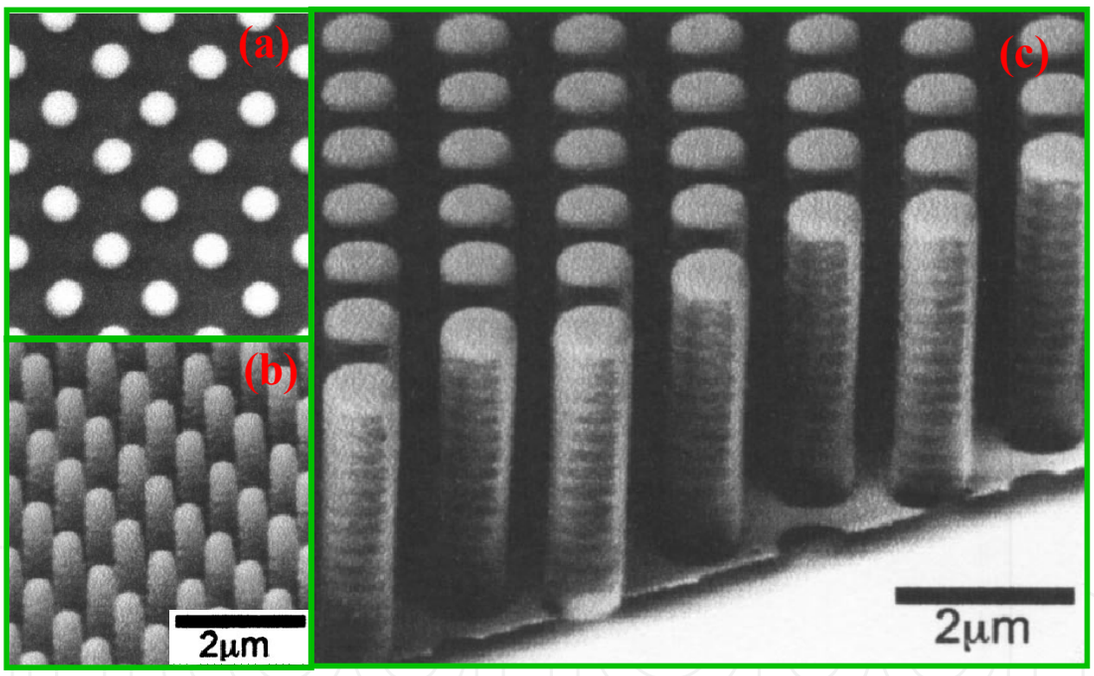


Figure 14. (a)(b) Top view and oblique view SEM images of the structure fabricated by the four-beam interference of fs pulses, (c) Close-up view of rods in the structure fabricated by four-beam interference of fs pulses with an interference angle of 21.9°.

Femtosecond pulses from a Ti:sapphire regenerative amplifier (wavelength of 800 nm, pulse duration of 150 fs, repetition rate of 1 kHz) were used for experiments. By using this method, periodic structures were fabricated. Periodic structures fabricated with an interference angle of 33.6° are presented in Fig. 14. In this figure, (a) and (b) show SEM images of the same sample from different perspectives. The oblique view shown in (b) clearly demonstrates that the periodic structure consists of high-aspect-ratio rods. The height and diameter of the rods are about 4 μm and 0.6 μm, respectively; thus, an aspect

ratio of about 7 was achieved. It should be noted that the height of the obtained structure is not limited by the coherent length of the pulse. A higher structure could be obtained if the stiffness of the material allowed the rods to withstand capillary forces during the development procedure.

Figure 14 (c) provides a close-up view of the rods fabricated with an interference angle at 21.9°. To obtain this image, the coverglass containing the fabricated structures was deliberately broken and a small fragment was observed. As seen, the rods are slightly bellows-shaped. Distinct ring-like features repeat periodically along each rod with a period about 0.3μm. This could be attributed as the result of interference between the incident and reflected beams at the resist–coverglass interface.

4. Conclusion

In conclusion, we have reviewed the fabrications of the one-dimensional and two-dimensional periodic microstructures on the surface or inside of materials by multiphoton absorption using a single shot of two or multiple interfered femtosecond laser pulses.

Firstly, we have introduced the fabrication of the micrograting by a single shot of two interfered femtosecond laser pulses. When two interfered pulses overlapped on the surface of the silica glass, not only did we get the ordinary grating whose periods accorded with the theoretic equation $d=\lambda/[2\sin(\theta/2)]$, but also obtained the extraordinary grating whose period is a half of the ordinary grating. The formation of the modulation grating could be attributed to the higher-order modulation arising from second-harmonic generation (SHG) when the femtosecond laser pulse was incident to the surface of silica glass. The multiple layers of the microgratings have been fabricated in the different depths of the silica glass sample by a single shot of two interfered femtosecond laser pulses, and the results show that the fabricated gratings can be read out by one of the recorded beams very easily. The noble metal nanoparticles consisted microgratings have also been realized in silicate glasses by two interfered femtosecond laser pulses with the aid of heat treatment because the noble metal nanoparticles in silica glass can be precipitated after the irradiation of the femtosecond laser and the successive heat treatment. At the same time, the multiple gratings can also be realized on the surface of the silica glass samples by a single shot of two interfered femtosecond laser pulses with the aid of a mask, which is very significative for enhancing the processing efficiency of the fabricated microgratings.

Secondly, we have also introduced the fabrication of the 1-D or 2-D periodic microstructures by a single shot of multiple interfered femtosecond laser pulses. When a single shot of three coplanar interfered femtosecond laser pulses interfered with each other on the surface of the silica glass, M-shaped gratings can be formed and the morphologies of the M-shaped gratings can also be modulated by tuning the incident pulse energy. However, when a single shot of noncoplanar three or four pulses interfered with each other, two-dimensional periodic microstructure can be obtained, which distributed as a hexagonal lattice. Different morphologies of the induced structures such as microvoid, orbicular platform and nanotip,

could be formed with the changes of the incident pulse energy. The fabrication of the 2D tetragonal lattice have also been fabricated in Negative photoresist SU-8 by four noncoplanar interfered pulses originating from the single pulse with the aid of the special DBS (diffractive beam splitter). Although the special DBS provided an easy way for realizing multiple beams interference, it also had some shortages, such as difficulty for fabricating microstructure with a smaller period, especially in the materials with big bandgap, such as silica glass.

Author details

Zhongyi Guo*
School of Computer and Information, Hefei University of Technology, Hefei, China
Department of Optoelectronic Science, Harbin Institute of Technology at Weihai, Weihai, China
Department of Physics, Harbin Institute of Technology, Harbin, China

Lingling Ran
Department of Optoelectronic Science, Harbin Institute of Technology at Weihai, Weihai, China
College of Electronic Engineering, Heilongjiang University, Harbin, China

Yanhua Han and Shiliang Qu
Department of Optoelectronic Science, Harbin Institute of Technology at Weihai, Weihai, China

Shutian Liu
Department of Physics, Harbin Institute of Technology, Harbin, China

Acknowledgement

This work was supported by the National Science Foundation of China (NSFC: 10904027; 61108018), the China Postdoctoral Science Foundation (AUGA41001348) and the Heilongjiang Province Postdoctoral Science Foundation (AUGA1100074), and development program for outstanding young teachers in Harbin Institute of Technology, HITQNJS. 2009. 033.

5. References

[1] C. Schaffer, A. Brodeur, J. García, and E. Mazur, "Micromachining bulk glass by use of femtosecond laser pulses with nanojoule energy," Opt. Lett. 26, 93-95 (2001)
[2] J. Koch, F. Korte, T. Bauer, C. Fallnich, A. Ostendorf, B. Chichkov. Nanotexturing of Gold Films by Femtosecond Laser-induced Melt Dynamics. Appl. Phys. A. 2005, 81:325–328.
[3] S. Juodkazis, H. Misawa, T. Hashimoto, E. Gamaly, and B. Luther-Davies, Laser-induced microexplosion confined in a bulk of silica: Formation of nanovoids, *Appl. Phys. Lett.* 88 (2006), 201909

* Corresponding Author

[4] Y. Li, Y. Dou, R. An, H. Yang, and Q. Gong,, "Permanent computer-generated holograms embedded in glass by femtosecond laser pulses," *Opt. Express,* 13 (2005) 2433-2438.

[5] Q. Zhao, J. Qiu, X. Jiang, E. Dai, C. Zhou, and C. Zhu, "Direct writing computer-generated holograms on metal film by an infrared femtosecond laser," *Opt. Express,* 13 (2005) 2089-2092.

[6] Z. Guo, S. Qu, Z. Sun, and S. Liu, "Superposition of orbit angular momentum of photons by combined computer-generated hologram fabricated in silica glass with femtosecond laser pulses", *Chin. Phys. B.* 17 (2008) 4199.

[7] Z. Guo, S. Qu, S. Liu, Generating optical vortex with computer-generated hologram fabricated inside glass by femtosecond laser pulses, Optics Communications, 273, 2007, 286-289.

[8] Z. Guo, H. Wang, Z. Liu, S. Qu, J. Dai, and S. Liu, Realization of holographic storage on metal film by femtosecond laser pulses micromachining, Journal of Nonlinear Optical Physics and Materials, 18(4), 2009, 617-623.

[9] Z. Guo, W. Ding, S. Qu, J. Dai, and S. Liu, Self-assembled volume grating in silica glass induced by a tightly focused femtosecond laser pulses, Journal of Nonlinear Optical Physics and Materials, 18(4), 2009, 625-632.

[10] K. Zhou, Z. Guo, W. Ding, and S. Liu, Analysis on volume grating induced by femotosecond laser pulses, Opt. Express 18(13), 2010, 13640-13646.

[11] Y. Li，W. Watanabe, K. Yamada, T. Shinagawa, K. Itoh, J. Nishii, and Y. Jiang "Holographic fabrication of multiple layers of grating inside soda–lime glass with femtosecond laser pulses". *Appl.Phys.Lett,* 80 (2002) 1508.

[12] S. Qu, J. Qiu, C. Zhao, X. Jiang, H. Zeng, C. Zhu, and K. Hirao, "Metal nanoparticle precipitation in periodic arrays in Au_2O-doped glass by two interfered femtosecond laser pulses," *Appl. Phys. Lett.* 84, 2046-2048, (2005).

[13] Y. Han, S. Qu, Q. Wang, Z. Guo, and X. Chen, Controllable grating fabrication by three interfering replicas of single femtosecond laser pulse, Chinese physics B, 18, 5331, (2009).

[14] S. Qu, C. Zhao, Q. Zhao, J. Qiu, C. Zhu, and K. Hirao, One-off writing of multimicrogratings on glass by two interfered femtosecond laser pulses, Opt. Lett. 29, 2058 (2004).

[15] Z. Guo, S. Qu, L. Ran, and S. Liu, Modulation grating achieved by two interfered femtosecond laser pulses on the surface of the silica glass, Appl. Surf. Sci., 253, 8581, (2007).

[16] Z. Guo, S. Qu, Y. Han, and S. Liu, Multi-photon fabrication of two-dimensional periodic structure by three interfered femtosecond laser pulses on the surface of the silica glass, Optics Communications, 280, 23-26, (2007)

[17] Z. Guo, L. Ran, Y. Han, S. Qu, and S. Liu, "The formation of novel two-dimensional periodic microstructures by a single shot of three interfered femtosecond laser pulses on the surface of the silica glass", *Opt. Lett.* 33 (2008) 2383.

[18] T. Kondo, S. Matsuo, S. Juodkazis, and H. Misawa, "Femtosecond laser interference technique with diffractive beam splitter for fabrication of three-dimensional photonic crystals" *Appl.Phys.Lett.* 79 (2001) 725-727.

[19] T. Kondo, S. Matsuo, S. Juodkazis, V. Mizeikis, and H. Misawa, "Multiphoton fabrication of periodic structures by multibeam interference of femtosecond pulses," *Appl.Phys.Lett.* 82 (2003) 2758-2760.

[20] J. Si, Z. Meng, S. Kanehira, J. Qiu, B. Hua and K. Hirao, "Multiphoton-induced periodic microstructures inside bulk azodye-doped polymers by multibeam laser interference", *Chem. Phys. Lett.* 399 (2004) 276-279

[21] L. Z. Cai, X. L. Yang, and Y. R. Wang, "All fourteen Bravais lattices can be formed by interference of four noncoplanar beams," Opt. Lett. 27, 900-902 (2002)

[22] L. Z. Cai, X. L. Yang, and Y. R. Wang, "Formation of three-dimensional periodic microstructures by interference of four noncoplanar beams," J. Opt. Soc. Am. A 19, 2238-2244 (2002)

[23] Zhongyi Guo, Shiliang Qu, Shutian Liu, and Jung-Ho Lee, Periodic microstructures induced by interfered femtosecond laser pulses, Proc. of SPIE Vol. 7657 76570K-1, 2010.

[24] D. Von der Linde, H. Schulz, T. Engers and H. Schuler, Second harmonic generation in plasmas produced by intense femtosecond laser pulses, *IEEE J. Quantum Electron.* 28, 2388, (1992).

[25] Y. Shen, The Principles of Nonlinear Optics, Wiley, New York (1984) 553.

[26] U. Österberg and W. Margulis, "Dye laser pumped by Nd:YAG laser pulses frequency doubled in a glass optical fiber," Opt. Lett. 11, 516-518 (1986).

[27] S. Qu, C. Zhao, X. Jiang, G. Fang, Y. Gao, H. Zeng, Y. Song, J. Qiu, C. Zhu, and K. Hirao, Optical nonlinearities of space selectively precipitated Au nanoparticles inside glasses, Chem. Phys. Lett. 368, 352 (2003).

[28] H. B. Liao, R. F. Xiao, J. S. Fu, H. Wang, K. S. Wong, and G. K. L. Wong, "Origin of third-order optical nonlinearity in Au:SiO_2 composite films on femtosecond and picosecond time scales," Opt. Lett. 23, 388-390 (1998)

[29] J. Qiu, M. Shirai, T. Nakaya, J. Si, X. Jiang, C. Zhu, Space-selective precipitation of metal nanoparticles inside glasses, Appl. Phys. Lett. 81, 3040 (2002).

[30] James R. Adleman, Helge A. Eggert, Karsten Buse, and Demetri Psaltis, "Holographic grating formation in a colloidal suspension of silver nanoparticles," Opt. Lett. 31, 447-449 (2006).

[31] E. Valentin, H. Bernas, C. Ricolleau, and F. Creuzet, Ion Beam "Photography": Decoupling Nucleation and Growth of Metal Clusters in Glass, Phys. Rev. Lett. 86, 99 (2001).

[32] Y. Nakata, T. Okada, and M. Maeda, Fabrication of dot matrix, comb, and nanowire structures using laser ablation by interfered femtosecond laser beams, Appl. Phys. Lett. 81, 4239 (2002).

[33] Yan Li, Kazuhiro Yamada, Tomohiko Ishizuka, Wataru Watanabe, Kazuyoshi Itoh, and Zhongxiang Zhou, "Single femtosecond pulse holography using polymethyl methacrylate," Opt. Express 10, 1173-1178 (2002)

[34] G. Qian, J. Guo, M. Wang, J. Si, J. Qiu, K. Hirao, Holographic volume gratings in bulk perylene-orange-doped hybrid inorganic-organic materials by the coherent field of a femtosecond laser, Appl. Phys. Lett., 83 (2003), p. 2327

[35] S. Juodkazis, H. Misawa, T. Hashimoto, E. Gamaly, and B. Davies, Laser-induced microexplosion confined in a bulk of silica: Formation of nanovoids, Appl. Phys. Lett. 88, 201909 (2006).

[36] Y. Lu, S. Theppakuttai, and S. Chen, Marangoni effect in nanosphere-enhanced laser nanopatterning of silicon, Appl. Phys. Lett. 82, 4143 (2003).

[37] J. Eizenkop, I. Avrutsky, G. Auner, D. Georgiev, and V. Chaudhary, Single pulse excimer laser nanostructuring of thin silicon films: Nanosharp cones formation and a heat transfer problem, J. Appl. Phys. 101, 094301 (2007).

[38] S. Huang, Z. Sun, B. Luk'yanchuk, M. Hong, and L. Shi, Nanobump arrays fabricated by laser irradiation of polystyrene particle layers on silicon, Appl. Phys. Lett. 86, 161911 (2005).

[39] R. Piparia, E. Rothe, and R. Baird, Nanobumps on silicon created with polystyrene spheres and 248 or 308 nm laser pulses, Appl. Phys. Lett. 89, 223113 (2006).

[40] K. Kawamura, N. Sarukura, M. Hirano, N. Ito, and H. Hosono, Periodic nanostructure array in crossed holographic gratings on silica glass by two interfered infrared-femtosecond laser pulses, Appl. Phys. Lett. 79, 1228 (2001).

IntechOpen